Enhancing Lithium Recovery from Slag Through Dry Forced Triboelectric Separation: A Sustainable Recycling Approach

Article *in* Minerals · December 2024

DOI: 10.3390/min14121254

9 authors, including:

Mehran Javadi
Clausthal University of Technology
16 PUBLICATIONS **118** CITATIONS
SEE PROFILE

Cindytami Rachmawati
TU Bergakademie Freiberg
8 PUBLICATIONS **13** CITATIONS
SEE PROFILE

Annett Wollmann
Clausthal University of Technology
35 PUBLICATIONS **147** CITATIONS
SEE PROFILE

Joao Pedro Weiss
RWTH Aachen University
12 PUBLICATIONS **8** CITATIONS
SEE PROFILE

minerals

MDPI

Article

Enhancing Lithium Recovery from Slag Through Dry Forced Triboelectric Separation: A Sustainable Recycling Approach

Mehran Javadi [1,*], Cindytami Rachmawati [2], Annett Wollmann [1], Joao Weiss [3], Hugo Lucas [3], Robert Möckel [4], Bernd Friedrich [3], Urs Peuker [2] and Alfred P. Weber [1]

[1] Institute of Particle Technology, Clausthal University of Technology, 38678 Clausthal-Zellerfeld, Germany; annett.wollmann@tu-clausthal.de (A.W.); weber@mvt.tu-clausthal.de (A.P.W.)
[2] Institute of Mechanical Process Engineering and Mineral Processing, Technische Universität Bergakademie Freiberg, 09599 Freiberg, Germany; cindytami.rachmawati@mvtat.tu-freiberg.de (C.R.); urs.peuker@mvtat.tu-freiberg.de (U.P.)
[3] Institute of Process Metallurgy and Metal Recycling, RWTH Aachen University, 52056 Aachen, Germany; jweiss@metallurgie.rwth-aachen.de (J.W.); hlucas@metallurgie.rwth-aachen.de (H.L.); bfriedrich@ime-aachen.de (B.F.)
[4] Helmholtz Center Dresden-Rossendorf, Helmholz Institute Freiberg for Resource Technology, 09599 Freiberg, Germany; r.moeckel@hzdr.de
* Correspondence: mehran.javadi@tu-clausthal.de

Abstract: The increasing use of lithium-containing materials highlights the urgent need for their recycling to preserve resources and protect the environment. Lithium-containing slags, produced during the pyrometallurgical process in lithium-ion battery recycling, represent an essential resource for lithium recovery efforts. While multiple methods for lithium recycling exist, it is crucial to emphasize environmentally sustainable approaches. This study employs dry forced triboelectrification (FTC) to recover valuable components from slag powder, commonly known as engineered artificial minerals (EnAMs). The FTC method is used to change the charge of the target material and achieve a neutral state while other materials remain charged. The downstream electrostatic separator enables the charged particles to be separated from the target material, which in this study is lithium aluminate. The results show that the method is effective, and lithium aluminate can be successfully enriched.

Keywords: lithium-ion battery recycling; engineered artificial minerals (EnAMs); forced triboelectric charging (FTC); electrostatic separation

Citation: Javadi, M.; Rachmawati, C.; Wollmann, A.; Weiss, J.; Lucas, H.; Möckel, R.; Friedrich, B.; Peuker, U.; Weber, A.P. Enhancing Lithium Recovery from Slag Through Dry Forced Triboelectric Separation: A Sustainable Recycling Approach. *Minerals* **2024**, *14*, 1254. https://doi.org/10.3390/min14121254

Academic Editor: Sunil Kumar Tripathy

Received: 31 October 2024
Revised: 29 November 2024
Accepted: 8 December 2024
Published: 10 December 2024

1. Introduction

The recycling of critical technology elements such as alkali and transition metals, which are used in batteries, capacitors, magnets, and sensors [1–3], for example, still lacks efficient and environmentally friendly technologies. Studies also explore how recycling costs and environmental risks affect the sustainability of the process, specifically for lithium-ion batteries (LIBs), emphasizing the importance of material efficiency, recycling methods, and the use of clean energy [4–6]. Evidence shows that many of these elements are lost in pyrometallurgical metal recovery processes, as they end up in the slag rather than the main metal phase. One example of this is lithium from the recycling of lithium-ion batteries (LIBs) [7]. As part of Priority Program 2315 "Engineered Artificial Minerals (EnAM)—a geo-metallurgical tool to recycle critical elements from waste streams", the slag phase is being investigated as an important source of critical technology elements in a holistic approach [8]. When the slag solidifies, it either forms a homogeneous amorphous structure or crystals are formed. These crystals are called artificial minerals (EnAMs). The formation of EnAMs itself depends on the thermodynamics of the complex multi-component system of the slag and the processing conditions of the melt, e.g., the

temperature profile and gradient during solidification. After a processing step in the form of liberating the crystallites, the target component needs to be concentrated. In classic ore processing, this concentration step is realized by flotation [9]. However, on the one hand, this route has limited environmental friendliness due to the numerous chemical additives and water consumption [10,11]. On the other hand, the presence of elements such as manganese (Mn) can make recovery more complicated due to the dispersion between oxides and silicates, which are particularly unsuitable for flotation [7].

Unlike the increase of lithium-ion batteries (LIBs), which are crucial for powering electronics and electric vehicles, their recycling rate lags far behind their production. Various emerging recycling methods exist for lithium-ion batteries (LIBs), e.g., OnTo, Battery Resources, LithoRec, and Accurec processes [12]. These methods focus on recovering valuable components, such as cathode and anode materials, to align with the circular economy (CE) concept. However, several challenges persist. First, material losses remain significant, with some valuable elements like anode material, electrolytes, graphite, copper (Cu), nickel (Ni), and lithium (Li) not being fully recovered. Additionally, the materials recovered often require further processing before they can be reused in new batteries, adding complexity and resource consumption. Many of these recycling processes also rely on multiple external inputs, such as chemicals and reagents, which leads to waste generation and goes against the idea of minimizing waste in CE processes. The diversity of cathode chemistries adds more complexity, as different types of cathodes may require distinct processing conditions, increasing energy consumption and reducing the quality of the recovered components. Furthermore, the lack of standardization in battery chemistries complicates sorting and recycling efforts, making it challenging to process mixed battery types efficiently. Lastly, processing diluted mixtures and varying feed and product quality requires advanced simulation tools to optimize recycling and reduce material losses [12].

To overcome these challenges and ensure the long-term viability of LIB recycling, studies have been conducted to explore more sustainable methods that minimize resource consumption, reduce waste generation, and enhance the efficiency of material recovery.

Lu et al. developed sustainable recycling methods using ternary lithium-ion batteries, particularly the cathode material. In this process, invasive plants served as carbon feedstock in a pyrolysis process. This minimizes waste streams and the use of reagents while achieving high recovery rates [13,14]. Additionally, electrochemical processes offer greener alternatives for lithium-ion battery recycling due to their selectivity, lower toxicity, and reliance on aqueous solutions rather than aggressive chemicals. However, challenges remain, including integrating the process into existing battery production systems to enable a circular lithium economy and energy use [15].

Electrostatic separation is a dry processing method that utilizes triboelectric charging of powders to separate materials and can be used as an alternative solution to the challenges in lithium-ion battery (LIB) recycling. In triboelectric charging and electrostatic separation processes, materials become electrically charged through contact and separation. When two different materials come into contact and then are separated, electrons move from one material to the other based on each material's work function (WF) [16]. This electron transfer causes one material to gain a positive charge and the other to gain a negative charge [16,17]. The charged particles are then exposed to an electric field, which acts as a separator to recover the target material from the gangue based on the material's triboelectric charging properties.

This technique is commonly used in recycling industries with industrial-scale separators to enhance mineral processing applications, such as fly ash beneficiation [18], separating quartz from feldspar [19], and removing silicates from phosphate ores to improve the quality of phosphate for fertilizers [20]. Although factors like material properties, moisture, particle size, and electrode configuration have been studied for their impact on separation, electrostatic separation is still not fully understood in the context of mineral processing [21]. Research has been conducted to evaluate how effectively this method

separates target materials from other minerals, with a focus on understanding charging behavior and improving enrichment [22]. Studies have also shown the influence of factors such as surface properties, environmental conditions, and contact charging [23], as well as the use of different tribochargers to enhance target material recovery [24]

This paper presents triboelectric charging and electrostatic separation as an environmentally friendly sorting and recovery technique that requires no additives. It is based on the distinct triboelectric charging behaviors of different slag components. A challenge in triboelectric charging is the existence of surface roughness, which results in the formation of bipolar charge distributions within each particle size class [25]. This causes an issue in the accumulation of materials due to a phenomenon known as equal mobility.

The novel approach presented here to address this issue is called forced triboelectric charging (FTC). Unlike natural charging, FTC shifts the target powder to a neutral charge state by applying a high voltage (HV) to the contacting wall (copper chute), where "forced" refers to the externally applied high voltage. The FTC technique was employed to recover lithium aluminate from Li-Slag. Charged particles are then introduced into an electrostatic separator for sorting. While so far this approach has only been applied for mixtures of pure powders (lithium aluminate/talcum [26] and Saxolith/Talcum[27]), here the recovery of lithium aluminate from real EnAM Li-Slag is addressed. This Li-Slag is more complex in regard to mixed crystalline phases, intergrowth, and compositions, which is especially challenging for the liberation of the target component. However, this method has the potential to optimize mineral processing by offering a dry, chemical-free separation that is both efficient and environmentally sustainable.

2. Materials and Methods

In the experiments, slag containing lithium aluminate, known as Li-Slag, was used with the goal of enriching the lithium aluminate component. Pure lithium aluminate powder was utilized as the target material to investigate its charging behavior. Li-Slag was produced in a pyrometallurgical process starting with known compositions, as detailed in the following sections. After solidification and comminution of the slag, powder with the size distribution shown in Table 1 (including pure lithium aluminate) was obtained. The mineral composition of the Li-Slag is detailed in Table 2.

Table 1. Characteristics (density measurement by gas pycnometer, size distribution measured by laser diffraction given as percentile) and origin of the used powder materials.

Powder Material	Supplier	Density ($g\ cm^{-3}$)	Particle Size (μm)		
			(x_{10})	(x_{50})	(x_{90})
Li-Slag (Multiple minerals)	IME-Institute of Process Metallurgy and Metal Recycling—RWTH	3.21	27	75	106
Lithium Aluminate	Sigma Aldrich Chemie GmbH	2.62	7.7	38	74

Table 2. Quantitative analyses of the Li-Slag in wt.% of the formed phases.

Components	Lithium Aluminate ($LiAlO_2$)	Mn-Al Spinel ($MnAl_2O_4$)	Gehlenite ($Ca_2Al_2SiO_7$)	Li_2MnSiO_4	Eucryptite ($LiAlSiO_4$)
Wt.%	8.2	36.1	31.7	13.8	9.1

The main crystalline phases identified are Gehlenite ($Ca_2Al_2SiO_7$), Mn-Al spinel ($MnAl_2O_4$), lithium aluminate ($LiAlO_2$), lithium manganese silicate (Li_2MnSiO_4), and eucryptite ($LiAlSiO_4$). By confirming the presence and quantity of lithium aluminate, XRD ensures that recycling efforts are accurately targeted toward the appropriate material.

2.1. Slag Production

Li-Slag was produced at IME RWTH Aachen using the feed components that consisted of 8.5% Li_2O, 10.4% MnO, 45.3% Al_2O_3, 16.9% CaO, and 18.9% SiO_2. The methodology and feed compositions were identical to those employed in a previous study [8]. In this study, the artificial slag was produced to provide a synthetic material promoting the formation of valuable phases. The primary phase of interest was lithium aluminate, identified as a stable and recoverable phase within the lithium slag. The compounds were heated up to 1500 °C, and successively, the molten slag was kept at this temperature for 5 h for homogenization. After the holding time, the controlled cooling procedure was started as the slag was firstly cooled down to 1050 °C and then kept at this temperature for another 6 h. This holding time serves to create a better solidification process and homogenization of the slag and increases the grain size regarding the lithium aluminate phases. Subsequently, the slag was again controlled and cooled down to room temperature. The cooling temperature rate used for the slag production was 25 °C h^{-1}.

2.2. Liberation of Lithium Aluminate

After producing the slag blocks, the blocks are cut into smaller pieces to prepare for the next stage. The small pieces are crushed and milled into fine slag powder using a jaw crusher and a ball mill combined with a screen of 100 µm mesh size. The powder is then divided using a rotary splitter to get a uniform and representative sample. Then, surface liberation, which refers to the amount of exposed target particle surface free from non-target materials (gangue), was conducted. In the triboelectric charging method, particles are charged according to their surface materials, making surface liberation important. This process entails additional crushing or grinding of the slag to diminish particle size, thus enhancing the surface area accessible for triboelectric interactions. Figure 1a shows the comminution process used to liberate grains from slag samples. Figure 1b indicates that a particle is considered fully liberated when its entire surface area consists of the target material, regardless of the presence of other components. In this study, particles with a free surface area (FSA) of 90%–100% are considered suitable for the separation process [28–30].

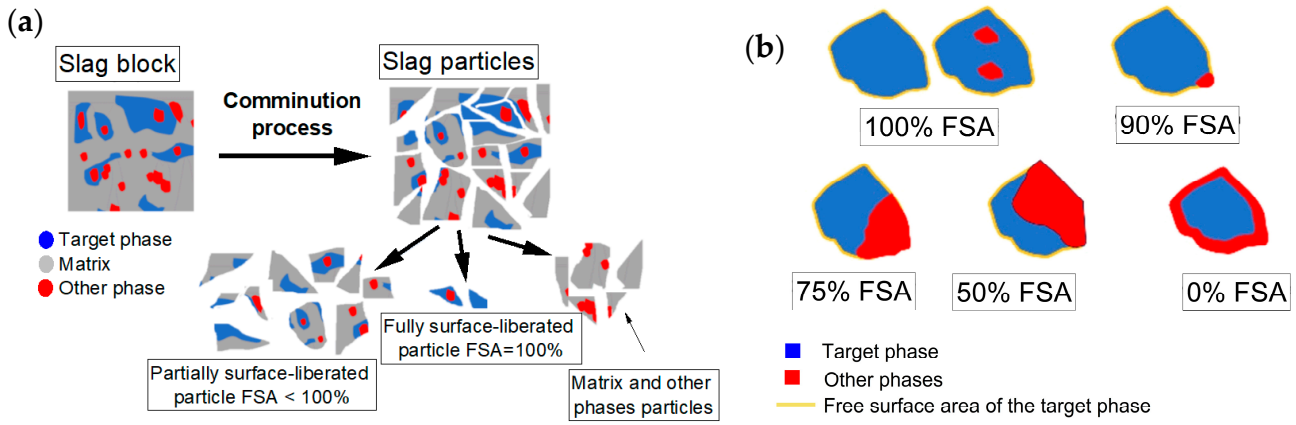

Figure 1. Schematic of (**a**) liberation by comminution (crushing and grinding), (**b**) slag components liberated to various degrees of free surface area (FSA) (partially and fully surface-liberated target phases).

2.3. Characterizing of Materials

To analyze the lithium slag powder, X-ray diffraction (XRD) identifies minerals by examining X-ray scattering patterns, revealing different crystalline phases. Lithium aluminate liberation was analyzed using automated mineralogy through mineral liberation analysis (MLA) with SEM-EDX-based measurements. A detailed explanation of the method can be found in [31]. The measurement of the liberation was based on the area ratio of the liberation grade of the target phase to the total area of the grain (Figure 1). To

measure the amount of lithium aluminate from sampled powder after the separation process, the collected powders were analyzed using the conductivity method and using a conductivity device (Windaus-Labortechnik GmbH, Clausthal-Zellerfeld, Germany). The conductivity of pure Li-Slag powders, which contain some lithium aluminate, was measured multiple times, represented as the axis intercept on the calibration line and defined as background value. Then, mixtures of Li-Slag and lithium aluminate with mass fractions of 0 to 20% were prepared, and their conductivities were measured at a constant temperature of 23 °C. A calibration curve was created from this, enabling the determination of lithium aluminate content in unknown samples (Appendix A).

2.4. Triboelectric Charging and Electrostatic Separation

2.4.1. FTC Process

After Li-Slag powder preparation, the triboelectric charging and electrostatic separation processes were conducted as the final steps to recycle lithium aluminate. Figure 2a illustrates the setup designed to measure the particle charge generated through FTC. In our former studies [27], operational parameters such as chute length (L), mass flow rate ($\dot{m}$), and inclination angle (α) in electrostatic sorting were investigated to optimize the charging of limestone particles. The optimum parameters from the study were transferred to the present investigation, i.e., chute length of 1000 mm and constant feed rate of 0.53 g.min^{-1}. A home-built feeder was used to control the mass flow rate of powders onto the chute. The applied voltage on the chute was varied from -12 to +12 kV using a high-voltage power supply (Heinzinger, PNC 30000-5). Additionally, a vibrator device (VIBRI®, Sympatec GmbH, Germany) was used to enhance powder flow on the chute surface. Charged particles on the chute were collected in an in-house designed Faraday Cup Electrometer (FCE) to measure the current over a certain time and to deduce the powder charge by integrating the current over this time. The FCE measurements were conducted using an electrometer (Keithley 6514, Cleveland, USA). By adjusting the high voltage, the point of zero net charge (PZNC) is determined, representing the point at which the average charge of the powder is zero. The specific charge was obtained from the ratio of powder charge to the collected mass in the FCE (in μC g^{-1}). Since environmental conditions such as relative humidity and temperature can affect the PZNC and WF, constant environmental parameters were maintained by conducting all experiments in a controlled and closed laboratory environment. Moreover, in our former study, the setup parameters, including the chute length, the mass flow rate of feed powder, and the chute incline angle, were investigated to understand their effects on the overall charging performance [27].

To separate the target material from the gangue, the charging behavior of the Li-Slag and pure lithium aluminate have to be analyzed first. Then, the voltage for PZNC of the target component is applied to the chute to recover it in the electrostatic sorter as a neutral fraction (Figure 2b).

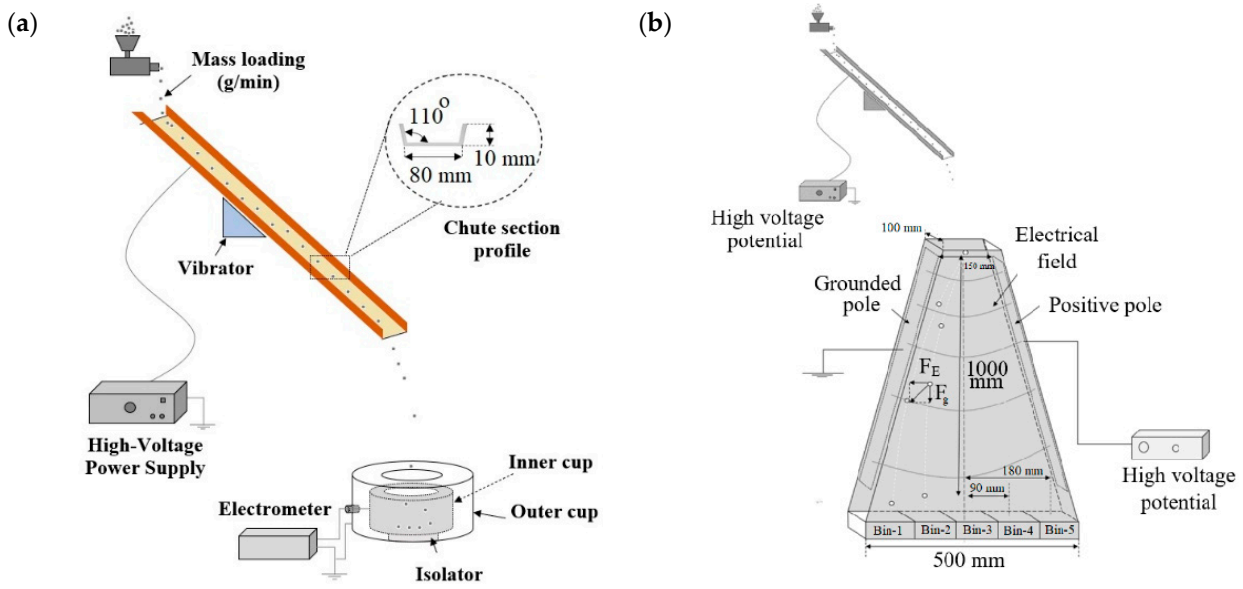

Figure 2. Experimental setup: (**a**) combination of dry forced triboelectric charging (FTC) of powders and the Faraday cup electrometer (FCE) test to determine the PZNC of the used materials and (**b**) the electrostatic separator, including five collection bins at the bottom**.**

2.4.2. Electrostatic Separation of Charged Particles

Following the triboelectric charging process, the charged particles are fed into an electrostatic separator. Within this separator, particles are classified according to their polarity and the amount of charge they carry, as investigated for different materials in our recent studies [26,27]. Figure 2b shows the separator setup, which includes two electrodes, one subjected to a high voltage of up to +25 kV while the other is grounded. To collect post-separation samples, a set of five identical rectangular bins labeled from 1 to 5 were used. These bins were positioned in a way that the middle one (bin 3) was aligned with the vertical axis of the chute outlet.

2.4.3. Free Fall Test

Free fall tests are conducted for both Li-Slag and lithium aluminate powders to assess their movement in the absence of the electrical field. These tests establish a baseline trajectory, showing the mere settling and dispersion behavior of particles under gravity alone. In these tests, powders are introduced into the chute and subsequently into the separator without any applied voltages (chute voltage: 0 kV, separator voltages: 0 kV). From these tests, it is possible to evaluate the effect of an electrical field on the lateral displacement of the particles.

3. Results

3.1. Material Preparation and Analysis

Figure 3a illustrates the Li-Slag body before it undergoes the comminution process. Initially, 125 kg of synthetic lithium slag was produced.

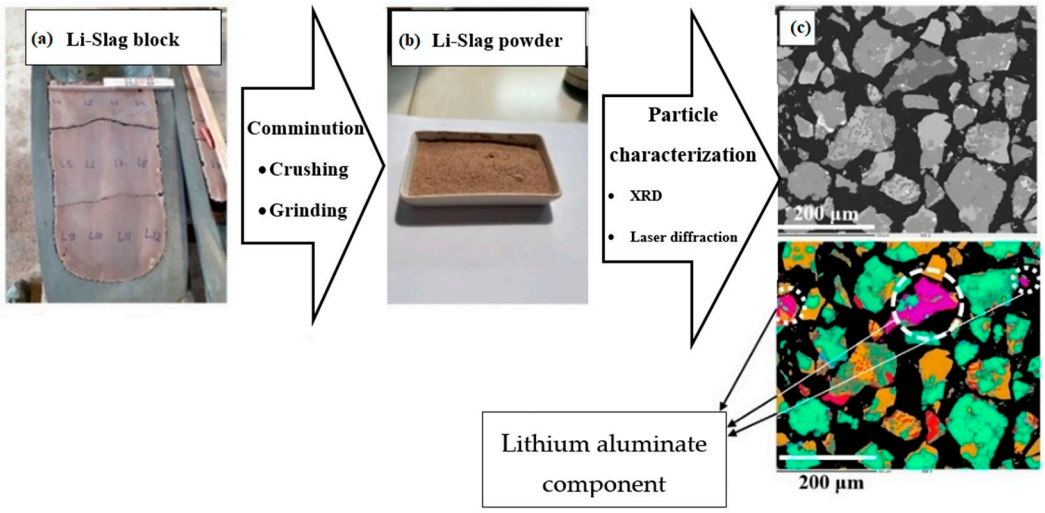

Figure 3. Slag transformation from (**a**) solid block to (**b**) powder form and (**c**) mineral characterization using an electron probe micro-analyzer (EPMA).

The particle size distribution of Li-Slag is shown in Figure 4a, obtained from MLA. The mineralogical composition of the slag, identified using X-ray diffraction analysis, is shown in Table 2. To quantify the phases, a Rietveld analysis was performed with the open-source software Profex/BGMN, version 5.1.0, which is effective for detecting Li-bearing phases in the slag [8].

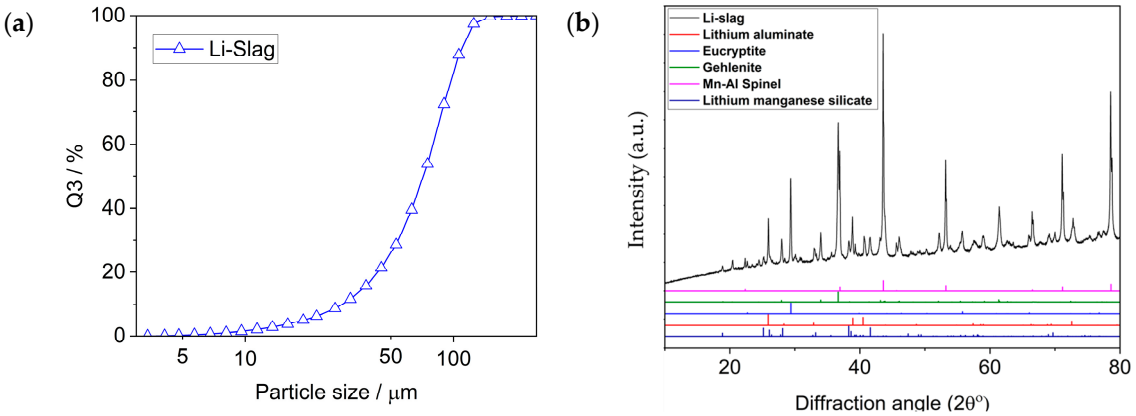

Figure 4. (**a**) Particle size distribution of Li-Slag obtained by MLA and (**b**) X-ray diffraction (XRD) pattern of Li-Slag and single-phase components [8].

To analyze the lithium aluminate liberation in Li-Slag powder, automated mineralogy using MLA with SEM-EDX-based measurements was carried out. Although the sample contains 8% lithium aluminate (Table 2), the 90%–100% liberation class only accounts for about 1% of the total sample mass in the milled slag (Figure 5b). Figure 5a displays particles containing a lithium aluminate mixture with varying degrees of liberation. In this figure, the pink regions represent lithium aluminate, while the other colors indicate different components. The fraction with the highest FSA in Figure 5b can be deconvoluted into different size classes (Figure 5c).

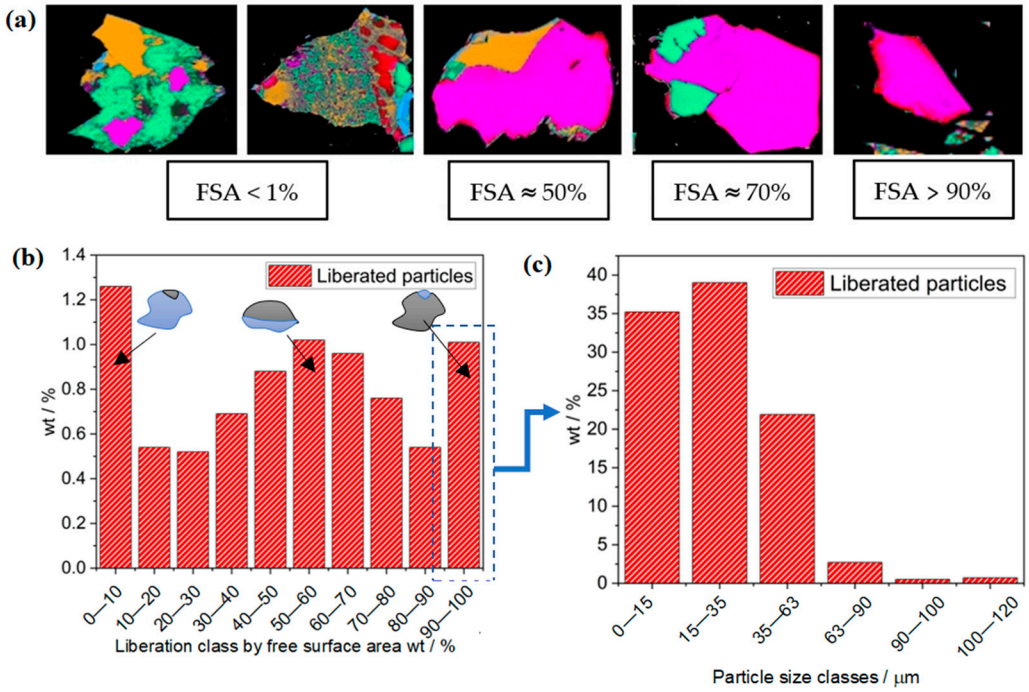

Figure 5. Characterization of the liberation of the lithium aluminate component in the Li-Slag: (**a**) examples of particles extracted from EPMA analysis (from Figure 3c, lithium aluminate in pink color) exhibiting different degrees of FSA, (**b**) lithium aluminate percentage in each liberation class by free surface area, and (**c**) particle size classes in the 90%–100% liberation class by free surface area.

In this study, particles with an FSA of 90%–100%, as shown in Figure 5b, are considered suitable for efficient sorting.

After the comminution of slag powder, only a minor fraction of the total lithium aluminate is fully liberated, reflecting a liberation efficiency of 1.1% (cf. Figure 5b). The size distribution of these fully liberated particles indicates that a substantial portion (35%) falls within the 0–15 micron range, with an additional 37% in the 15–35 micron range (cf. Figure 5c). Most of the liberated lithium aluminate is present as fine particles, resulting in several processing challenges. In the charging process, these small particles are more sensitive to environmental conditions, and in the separation step, they require longer settling times within the electrical field due to their small size and low mass.

3.2. Charging Behavior of Used Materials

With regard to the electrostatic separation of the powders, the charging behavior of each component must first be characterized. Therefore, pure lithium aluminate, in addition to Li-Slag, was also used in these experiments to assess the triboelectric charging properties of the target material. Figure 6 illustrates the charging behavior of Li-Slag, lithium aluminate, and their mixture. The graph presents the mass-specific charge of the powders as a function of the voltage applied to the chute (-12 to +12 kV).

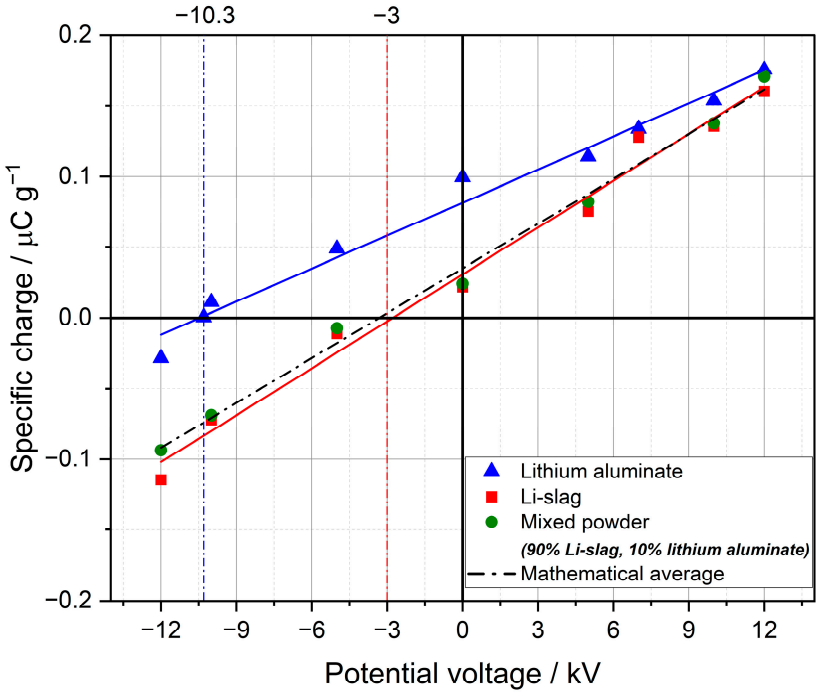

Figure 6. The specific charge of powders as a function of the applied voltage in the range of -12 to +12 kV for pure lithium aluminate, Li-Slag, and their mixture (10%/90%). From the fits of the two powders, the charging behavior of the mixture was calculated as a weighted average (black dashed line), which agrees very well with the measurements (green points).

Without applying a voltage to the chute, lithium aluminate and Li-Slag powders are positively charged. When a negative high voltage is applied to the chute, electrons transfer from the copper to the powder, reducing the positive particle charge. Finally, by applying a certain negative voltage, the powders reach the neutral state on average (PZNC). The PZNC corresponds to −10.3 kV for lithium aluminate, while the PZNC of Li-Slag is found at −3 kV. This shows that at the PZNC of the target material, the rest of the powder carries a charge of −0.08 µC g^{-1}. In turn, at the PZNC of Li-Slag, the target material is positively charged (+0.06 µC g^{-1}). For physically mixed powder (10:90 mixtures of lithium aluminate and Li-Slag), a simple superposition of the specific charge of the individual components is observed. This shows that the triboelectric charging of mixtures can be treated as the sum of the individual powder components, which is the prerequisite for material-specific sorting, supposing that the target component is fully liberated (FSA ≈ 90%–100%).

Particles that are not fully liberated (FSA < 90%) may contribute to charging behavior and to the lithium aluminate detection by conductivity measurements. However, in the first approach, this possible interference effect will be neglected in the following.

3.3. Electrostatic Separation

3.3.1. Free Fall Test

Free fall tests are conducted to assess the movement of the small particles in the absence of the electrical field. Figure 7 shows the mass fractions of Li-Slag and lithium aluminate powders from free fall tests. In Figure 7a, about 93% of the Li-Slag powder mass is found in bin 3, with smaller amounts of 5% in bin 2 and 2% in bin 4, respectively. Figure 7b illustrates that approximately 92% of the lithium aluminate powder mass is collected in bin 3, with the remaining particles in bin 2 (4.5%) and bin 4 (3.5%).

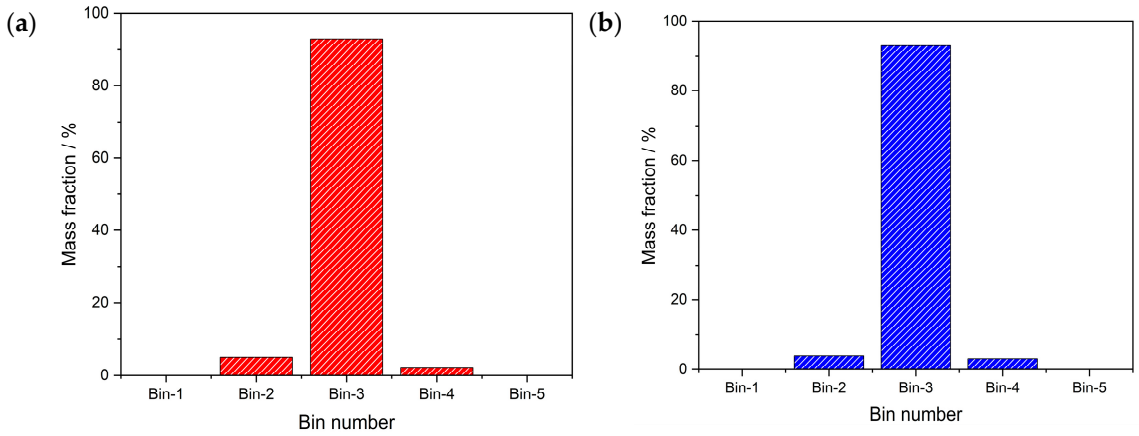

Figure 7. Free fall test of (**a**) Li-Slag and (**b**) lithium aluminate powders, demonstrating particle settling behavior through the separator without applied voltages (V_{chute} = 0 kV, V_{sep} = 0 kV).

This shows that the particle motion without the electrical field in the sorter is dominated by gravity. When a voltage is applied at the electrostatic separator, particle deposition in bin 1 and bin 5 is attributed to the electrical migration of charged particles. In fact, the charge distribution can be deduced from the lateral displacement and the particle size distribution in different bins. In former experiments, a charge distribution was found even at the PZNC for the material Saxolith; depending on the particle size, i.e., charge distributions containing positive and negative branches, the width of the charge distribution increases with the particle size [27].

As previously noted, the mass fraction of the fully liberated target material, lithium aluminate, is quite low. Therefore, the electrostatic sorting is initially performed on pure Li-Slag, which contains approximately 1% of fully liberated lithium aluminate (FSA ≈ 90%–100%). Subsequently, pure lithium aluminate is added to the Li-Slag powder to achieve a final mixture composed of 10% fully liberated lithium aluminate and 90% Li-Slag, allowing for a clearer evaluation of the sorting process's performance. This higher concentration helps to validate the effectiveness of the electrostatic sorting method and facilitates comparative analysis with results from pure Li-Slag and mixture.

3.3.2. Electrostatic Separation of Li-Slag

To explore the sorting behavior of Li-Slag and lithium aluminate, PZNC values of −3 kV (PZNC Li-Slag) and −10.3 kV (PZNC lithium aluminate) were applied to the chute. Figure 8 illustrates the results obtained from analyzing samples collected from five bins during this process. As shown in Figure 8a, when a voltage of −3 kV is applied to the chute, lithium aluminate, which is, on average, slightly positively charged at this voltage, tends to move towards the negative pole, depleting bin 5 (0.12%). Bin 4 has a slightly higher concentration of lithium aluminate of around 0.51%, which may be explained by the influence of only partially liberated particles since the sum of lithium aluminate in all bins (1.67%) is higher than the fraction of fully liberated lithium aluminate particles (1.1%). This demonstrates that when a voltage other than the PZNC of lithium aluminate is applied, both fully liberated and partially liberated lithium aluminate crystals are influenced by the applied voltage.

In Figure 8b, when the chute voltage is set to the PZNC for lithium aluminate at −10.3 kV, there is some enrichment of lithium aluminate (by a factor of 1.4, from 0.56% to 0.78%) in bin 3.

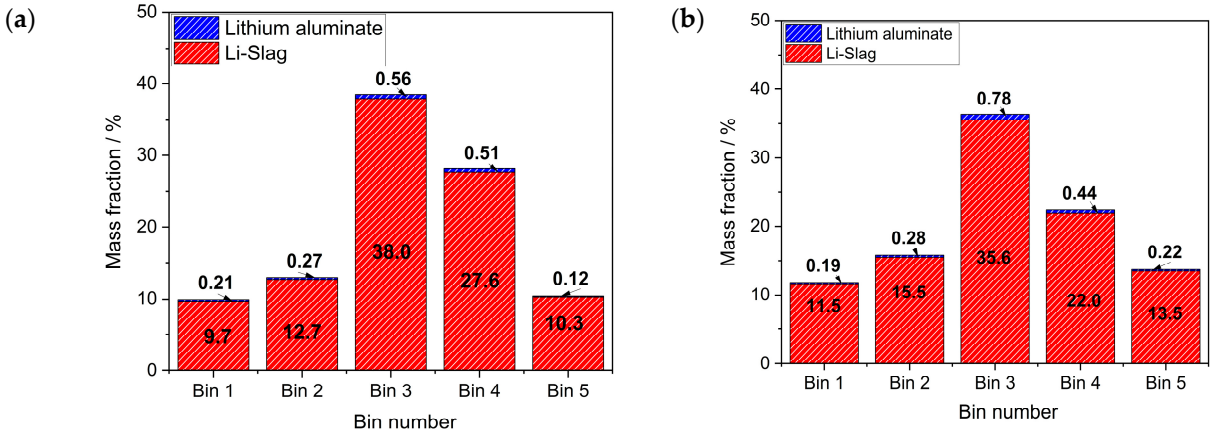

Figure 8. Electrostatic separation of original Li-Slag (**a**) at −3 kV (PZNC of Li-Slag) and (**b**) at −10.3 kV (PZNC of lithium aluminate). The numbers in the figure give the mass fraction of lithium slag (red) and of lithium aluminate (blue) (the sum of a mass fraction over all bins accounts for 100%).

The enrichment shown in Figure 8b is marginal and may suffer from uncertainties in conductivity measurement. While the concentration of lithium aluminate, the target material, was successful, recovery was limited due to incomplete liberation of its free surface area. Therefore, to better assess the enrichment process, the percentage of lithium aluminate was increased to 10% by adding pure lithium aluminate (cf. Table 1) to the Li-Slag powder.

3.3.3. Electrostatic Separation of Mixed Powder

The tests were then repeated using a mixture of 90% Li-Slag and 10% lithium aluminate. Figure 9a shows that when the PZNC voltage of Li-Slag is applied to the chute, Li-Slag particles attain an average specific charge of zero, while lithium aluminate particles remain charged (cf. Figure 6). These charged lithium aluminate particles are then attracted to different poles depending on their charge polarity. In this setup, bin 3, which is positioned at a neutral point, contains about 0.8% lithium aluminate. When switching to the PZNC of lithium aluminate, a substantial enrichment in bin 3 by almost a factor of 5 for the target component is reached (Figure 9b). The enrichment of lithium aluminate can substantially be improved when the fraction of particles with high FSA values is increased. Therefore, future work should address optimizing the solidification process of the slag (cooling rates, additives, etc.) [32], leading to larger target material grains, which can be liberated with a higher FSA content by comminution. This approach would also improve the liberation process, leading to better recovery of the target component.

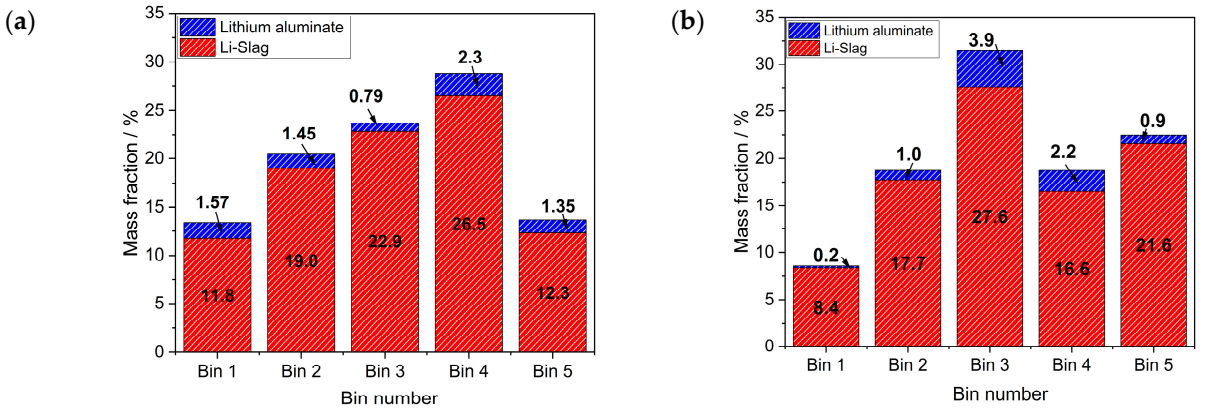

Figure 9. Electrostatic separation of the mixture of Li-Slag and lithium aluminate (**a**) at −3 kV (PZNC of Li-Slag) and (**b**) at −10.3 kV (PZNC of lithium aluminate). The numbers in the figure show the mass fraction of lithium slag (red) and lithium aluminate (blue).

To enhance the degree of enrichment and optimize the separation efficiency of slag, the primary challenge is to promote the growth of individual lithium aluminate crystals. Crystal growth can be enhanced by controlling temperature and cooling rates during crystallization [33] or by adjusting other factors (e.g., additives) that influence crystal development. Increasing the size and purity of lithium aluminate crystals will facilitate more effective liberation during comminution processes. Optimizing the liberation efficiency of the target component will significantly improve the presented enrichment process (both charging and separation). These strategies are essential to increase the overall effectiveness of dry slag sorting.

4. Conclusions

This study investigated the production, liberation, and electrostatic separation processes of lithium aluminate from synthetic Li-Slag. The initial production involved meticulously comminuting 125 kg of slag into a finely milled powder characterized by X-ray diffraction to identify the component phases. Despite initial challenges with only about 1.1% liberation of lithium aluminate, the addition of lithium aluminate powder increased its concentration to 10%, facilitating improved concentration measurements and preparation for electrostatic separation, which is a combination of forced triboelectric charging (FTC) on a copper chute and electrostatic precipitation in an electrosorter with five bins.

Through the FTC method, it is possible to manipulate the powder's charge from one polarity to another, thereby passing a neutral state at a specific voltage (PZNC). This method allows the target component, such as lithium aluminate, to be selectively moved into a neutral state while the rest of the powder remains charged. Then, the sorting experiments at the PZNC of lithium aluminate show enrichment of this component in bin 3, where the neutral fraction is collected. The small concentration of the enriched component is affected by the low content of fully liberated target material in the pure Li-Slag, as shown by the addition of free lithium aluminum particles.

Author Contributions: Conceptualization, M. J., A.W., and A.P.W.; Data curation, M.J.; Formal analysis, M.J., A.W., and A.P.W.; Funding acquisition, U.P. and A.P.W.; Investigation, M.J., C.R., A.W., and R.M.; Methodology, M.J., C.R., A.W., R.M., and A.P.W.; Project administration, A.P.W.; Resources, M.J.; Supervision, U.P. and A.P.W.; Writing—original draft, M.J. and C.R.; Writing—review and editing, A.W., J.W., H.L., B.F., U.P., and A.P.W. All authors have read and agreed to the published version of the manuscript.

Funding: German Research Foundation (DFG), priority program PP2315 under the grant number (WE 2331/33-1).

Data Availability Statement: The data are available upon reasonable request from the corresponding author.

Acknowledgments: The authors would like to express their appreciation to the German Research Foundation (DFG) for their valuable financial support of this project as part of Priority Program PP2315. We also extend our thanks to Thomas Schirmer, Institute for Repository Research TU Clausthal, for his technical assistance and the micrographs with the electron probe micro-analyzer (EPMA).

Conflicts of Interest: The authors declare no conflicts of interest.

Appendix A

Figure A1 illustrates the conductivity of the mixed powder with different mass fractions of lithium aluminate. The resulting data show a linear increase in conductivity, ranging from approximately 67.4 μS cm^{-1} for the pure Li-Slag sample to 180.3 μS cm^{-1} for the sample containing 20% added lithium aluminate. This linear trend indicates a direct relationship between the fraction of lithium aluminate and the overall conductivity of the mixed powder. Then, samples collected from the bins (after separation) were subjected to

the conductivity test, and based on the conductivity, the mass fraction was obtained from the calibration diagram.

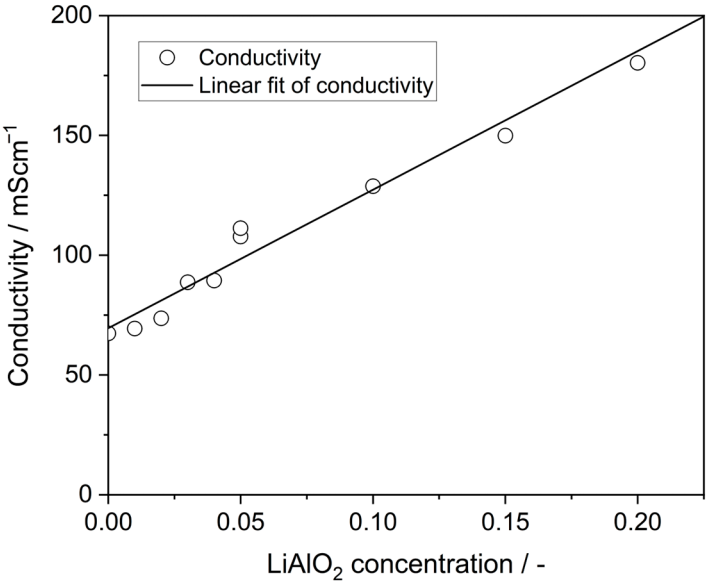

Figure A1. Conductivity of the mixture of Li-Slag and lithium aluminate for adding different amounts of lithium aluminate.

References

1. Lebrouhi, B.E.; Baghi, S.; Lamrani, B.; Schall, E.; Kousksou, T. Critical Materials for Electrical Energy Storage: Li-Ion Batteries. *J. Energy Storage* **2022**, *55*, 105471.
2. Liu, W.; Sun, X.; Yan, X.; Gao, Y.; Zhang, X.; Wang, K.; Ma, Y. Review of Energy Storage Capacitor Technology. *Batteries* **2024**, *10*, 271. https://doi.org/10.3390/batteries10080271.
3. Kaur, B.; Kaur, N.; Kumar, S. Colorimetric Metal Ion Sensors—A Comprehensive Review of the Years 2011–2016. *Coord. Chem. Rev.* **2018**, *358*, 13–69. https://doi.org/10.1016/j.ccr.2017.12.002.
4. Kaya, M. State-of-the-Art Lithium-Ion Battery Recycling Technologies. *Circ. Econ.* **2022**, *1*, 100015. https://doi.org/10.1016/j.cec.2022.100015.
5. Ambrose, H.; Kendall, A. Understanding the Future of Lithium: Part 1, Resource Model. *J. Ind. Ecol.* **2020**, *24*, 80–89. https://doi.org/10.1111/jiec.12949.
6. Lima, M.C.C.; Pontes, L.P.; Vasconcelos, A.S.M.; de Araujo Silva, W., Jr.; Wu, K. Economic Aspects for Recycling of Used Lithium-Ion Batteries from Electric Vehicles. *Energies* **2022**, *15*, 2203. https://doi.org/10.3390/en15062203.
7. Sommerfeld, M.; Vonderstein, C.; Dertmann, C.; Klimko, J.; Oráč, D.; Miškufová, A.; Havlík, T.; Friedrich, B. A Combined Pyro- and Hydrometallurgical Approach to Recycle Pyrolyzed Lithium-Ion Battery Black Mass Part 1: Production of Lithium Concentrates in An Electric Arc Furnace. *Metals* **2020**, *10*, 1069. https://doi.org/10.3390/met10081069.
8. Rachmawati, C.; Weiss, J.; Lucas, H.I.; Löwer, E.; Leißner, T.; Ebert, D.; Möckel, R.; Friedrich, B.; Peuker, U.A. Characterisation of the Grain Morphology of Artificial Minerals (EnAMs) in Lithium Slags by Correlating Multi-Dimensional 2D and 3D Methods. *Minerals* **2024**, *14*, 130. https://doi.org/10.3390/min14020130.
9. Wills, B.A. *Wills' Mineral Processing Technology: An Introduction to the Practical Aspects of Ore Treatment and Mineral Recovery*, 7th ed.; Elsevier Science & Technology: Oxford, UK, 2011; ISBN 978-0-7506-4450-1.
10. Falconi, I.B.A.; Botelho, A.B.; Baltazar, M.D.P.G.; Espinosa, D.C.R.; Tenório, J.A.S. An Overview of Treatment Techniques to Remove Ore Flotation Reagents from Mining Wastewater. *J. Environ. Chem. Eng.* **2023**, *11*, 111270. https://doi.org/10.1016/j.jece.2023.111270.
11. Aaltonen, A.; Izart, C.; Lyyra, M.; Lang, A.; Saari, E.; Dahl, O. Simulating the Impact of Ore and Water Quality on Flotation Recovery During the Life of A Mine. *Minerals* **2023**, *13*, 1230. https://doi.org/10.3390/min13091230.
12. Velázquez-Martínez, O.; Valio, J.; Santasalo-Aarnio, A.; Reuter, M.; Serna-Guerrero, R. A Critical Review of Lithium-Ion Battery Recycling Processes from a Circular Economy Perspective. *Batteries* **2019**, *5*, 68. https://doi.org/10.3390/batteries5040068.
13. Lu, J.; Zhang, Y.; Huang, W.; Omran, M.; Zhang, F.; Gao, L.; Chen, G. Reductive Roasting of Cathode Powder of Spent Ternary Lithium-Ion Battery by Pyrolysis of Invasive Plant Crofton Weed. *Renew. Energy* **2023**, *206*, 86–96. https://doi.org/10.1016/j.renene.2023.02.005.
14. Lu, J.; Tian, C.; Ren, C.; Omran, M.; Zhang, F.; Gao, L.; Chen, G. Priority Recovering of Lithium from Spent Lithium-Ion Battery Cathode Powder by Pyrolysis Reduction of Bidens Pilosa. *J. Clean. Prod.* **2024**, *439*, 140775. https://doi.org/10.1016/j.jclepro.2024.140775.

15. Xing, Z.; Srinivasan, M. Electrochemical Approach for Lithium Recovery from Spent Lithium-Ion Batteries: Opportunities and Challenges. *ACS Sustain. Resour. Manag.* **2024**, *1*, 1326–1339. https://doi.org/10.1021/acssusresmgt.4c00003.
16. Lang, N.D.; Kohn, W. Theory of Metal Surfaces: Work Function. *Phys. Rev. B* **1971**, *3*, 1215–1223. https://doi.org/10.1103/PhysRevB.3.1215.
17. Gupta, R.; Gidaspow, D.; Wasan, D.T. Electrostatic Separation of Powder Mixtures Based on the Work Functions of Its Constituents. *Powder Technol.* **1993**, *75*, 79–87. https://doi.org/10.1016/0032-5910(93)80027-8.
18. Ban, H.; Li, T.X.; Schaefer, J.L.; Stencel, J.M. Triboelectrostatic Separation of Unburned Carbon from Fly Ash. *Fuel Energy Abstr.* **1996**, *37*, 426. https://doi.org/10.1016/S0140-6701(97)83428-5.
19. Peretti, R.; Serci, A.; Zucca, A. Electrostatic K-Feldspar/Na-Feldspar and Feldspar/Quartz Separation: Influence of Feldspar Composition. *Miner. Process. Extr. Metall. Rev.* **2012**, *33*, 220–231. https://doi.org/10.1080/08827508.2011.563156.
20. Ruan, Y.; He, D.; Chi, R. Review on Beneficiation Techniques and Reagents Used for Phosphate Ores. *Minerals* 2019, *9*, 253. https://doi.org/10.3390/min9040253.
21. Dötterl, M.; Wachsmuth, U.; Waldmann, L.; Flachberger, H.; Mirkowska, M.; Brands, L.; Beier, P.-M.; Stahl†, I. Electrostatic Separation. In *Ullmann's Encyclopedia of Industrial Chemistry*; John Wiley & Sons, Ltd.: New York, NY, USA, 2016; pp. 1–35, ISBN 978-3-527-30673-2.
22. Gehringer, S.; Luckeneder, C.; Flachberger, H. Systematic Separation Studies on Finely Dispersed Raw Magnesite by Using Triboelectrostatic Belt Separation. *Berg Huettenmaenn Monatsh* **2020**, *165*, 364–368. https://doi.org/10.1007/s00501-020-01006-w.
23. Mirkowska, M.; Kratzer, M.; Teichert, C.; Flachberger, H. Principal Factors of Contact Charging of Minerals for a Successful Triboelectrostatic Separation Process—A Review. *Berg Huettenmaenn Monatsh* **2016**, *161*, 359–382. https://doi.org/10.1007/s00501-016-0515-1.
24. Yang, X.; Wang, H.; Peng, Z.; Hao, J.; Zhang, G.; Xie, W.; He, Y. Triboelectric Properties of Ilmenite and Quartz Minerals and Investigation of Triboelectric Separation of Ilmenite Ore. *Int. J. Min. Sci. Technol.* **2018**, *28*, 223–230. https://doi.org/10.1016/j.ijmst.2018.01.003.
25. Wei, J.; Realff, M.J. Design and Optimization of Free-Fall Electrostatic Separators for Plastics Recycling. *AIChE J.* **2003**, *49*, 3138–3149. https://doi.org/10.1002/aic.690491214.
26. Javadi, M.; Abohelwa, M.; Wollmann, A.; Weber, A.P. Dry Recycling of Lithium-Containing Material by Forced Tribocharging and Electrostatic Separation. *Chem. Ing. Tech.* **2024**, *96*, 950–957. https://doi.org/10.1002/cite.202300138.
27. Javadi, M.; Abohelwa, M.; Wollmann, A.; Weber, A.P. Characteristics of Powder Charging Behavior Via Forced Triboelectric Charging on An Inclined Chute. *Powder Technol.* **2025**, *449*, 120400. https://doi.org/10.1016/j.powtec.2024.120400.
28. Li, Z.; Fu, Y.; Yang, C.; Yu, W.; Liu, L.; Qu, J.; Zhao, W. Mineral Liberation Analysis on Coal Components Separated Using Typical Comminution Methods. *Miner. Eng.* **2018**, *126*, 74–81. https://doi.org/10.1016/j.mineng.2018.06.028.
29. Hirschberger, P.; Võ, T.T.; Peuker, U.; Kruggel-Emden, H. A Texture Inheritance Model for Spherical Particles in Particle Replacement Method (PRM) Schemes for Breakage in Discrete Element Method (DEM) Simulations. *Miner. Eng.* **2024**, *205*, 108491. https://doi.org/10.1016/j.mineng.2023.108491.
30. Wang, H.; Zhang, X.; Shen, L.; Yang, S.; Luo, L.; Song, S. Liberation and Enrichment of Metallic Iron from Reductively Roasted Copper Slag. *JOM* **2021**, *73*, 1013–1022. https://doi.org/10.1007/s11837-021-04570-9.
31. Schulz, B.; Sandmann, D.; Gilbricht, S. SEM-Based Automated Mineralogy and Its Application in Geo-And Material Sciences. *Minerals* **2020**, *10*, 1004. https://doi.org/10.3390/min10111004.
32. Chakrabarty, S.; Li, H.; Schirmer, T.; Hampel, S.; Fittschen, U.E.A.; Fischlschweiger, M. Non-Equilibrium Thermodynamic Modelling of Cooling Path Dependent Phase Evolution of Li_2SiO_3 from Li_2O-SiO_2 Melt by Considering Mixed Kinetic Phenomena and Time-Dependent Concentration Fields. *Scr. Mater.* **2024**, *242*, 115922. https://doi.org/10.1016/j.scriptamat.2023.115922.
33. Schnickmann, A.; De Abreu, D.A.; Fabrichnaya, O.; Schirmer, T. Stabilization of Mn4+ in Synthetic Slags and Identification of Important Slag Forming Phases. *Minerals* **2024**, *14*, 368. https://doi.org/10.3390/min14040368.